

# Learning from 2D: Contrastive Pixel-to-Point Knowledge Transfer for 3D Pretraining

Yueh-Cheng Liu<sup>1</sup>, Yu-Kai Huang<sup>1</sup>, Hung-Yueh Chiang<sup>2</sup>, Hung-Ting Su<sup>1</sup>, Zhe-Yu Liu<sup>1</sup>, Chin-Tang Chen<sup>1</sup>, Ching-Yu Tseng<sup>1</sup>, and Winston H. Hsu<sup>1</sup>

<sup>1</sup>National Taiwan University  
<sup>2</sup>The University of Texas at Austin

**Abstract**—Most 3D neural networks are trained from scratch owing to the lack of large-scale labeled 3D datasets. In this paper, we present a novel 3D pretraining method by leveraging 2D networks learned from rich 2D datasets. We propose the contrastive pixel-to-point knowledge transfer to effectively utilize the 2D information by mapping the pixel-level and point-level features into the same embedding space. Due to the heterogeneous nature between 2D and 3D networks, we introduce the back-projection function to align the features between 2D and 3D to make the transfer possible. Additionally, we devise an upsampling feature projection layer to increase the spatial resolution of high-level 2D feature maps, which enables learning fine-grained 3D representations. With a pretrained 2D network, the proposed pretraining process requires no additional 2D or 3D labeled data, further alleviating the expensive 3D data annotation cost. To the best of our knowledge, we are the first to exploit existing 2D trained weights to pretrain 3D deep neural networks. Our intensive experiments show that the 3D models pretrained with 2D knowledge boost the performances of 3D networks across various real-world 3D downstream tasks.

**Index Terms**—Pretraining, 3D neural network, 3D deep learning, contrastive learning

## I. INTRODUCTION

3D deep learning has gained a large amount of attention recently due to its wide applications, including robotics, autonomous driving, and virtual reality. Numerous state-of-the-art 3D neural network architectures have been proposed, showing remarkable performance improvements, including point-based methods [1]–[3], efficient sparse 3D CNN [4], [5], and hybrid point-voxel methods [6], [7]. However, unlike the well-established practice that uses large-scale datasets (*e.g.*, ImageNet [8]) to pretrain 2D neural networks for various applications, most of the 3D neural networks are trained from scratch. Although many efforts are made to collect 3D datasets [9]–[11], the expensive labeling cost and various 3D sensing devices make it challenging to build a large-scale dataset comparable to ImageNet, resulting in supervised pretraining in 3D difficult.

Recently, self-supervised pretraining has been proved successful in NLP [13], [14] and 2D vision [15]–[22] by using large unlabeled data to pretrain the neural networks. This direction is promising since it can easily scale-up without the need of human annotations. In 3D vision, PointContrast [12] first shows the opportunity of self-supervised pretraining by leveraging contrastive learning for point cloud data. By learning point correspondences across two partially-overlapping

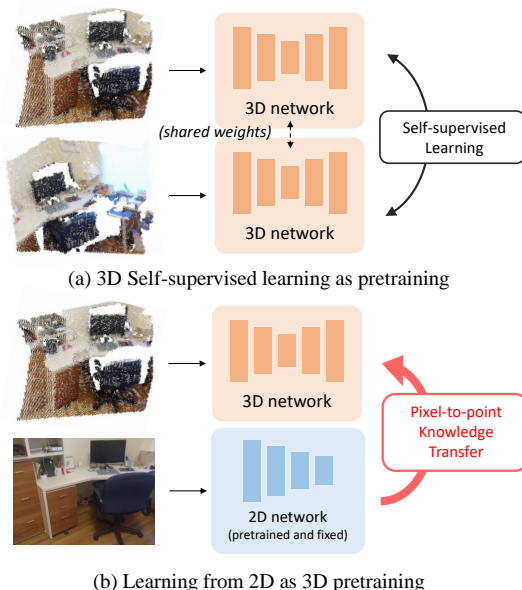


Fig. 1. **Learning from 2D as 3D pretraining.** Due to the limited size of 3D labeled data, 3D pretraining with large unlabeled data is critical. (a) Previous works [12] apply self-supervised learning on 3D as pretraining. (b) We propose pretraining 3D networks by leveraging the existing 2D network weights with our contrastive pixel-to-point knowledge transfer. In this way, we can provide the knowledge learned from rich 2D image datasets for the 3D networks as initial model weights.

point clouds, it can construct good initial weights for other 3D downstream tasks, such as 3D semantic segmentation and object detection.

In this work, we study pretraining 3D neural networks for point cloud data from a novel perspective – by learning from 2D pretrained networks (see Figure 1 for conceptual comparison). PointContrast [12] successfully brings the 2D self-supervised learning paradigm into 3D, but it neglects the 2D semantic information, for example, the semantic cue extracted by 2D CNN. Enormous 2D labeled datasets are much larger and more diverse than the 3D datasets, and the 2D network architectures have been widely studied and well developed in the past few years. Therefore, we believe that the knowledge of well-trained 2D networks is valuable and informative, which can provide the 3D network signals to learn good initial weights without additional labeled data. Our

idea is also related to previous 2D-3D fusion research [23]–[25], suggesting that features extracted by 2D networks can complement the 3D counterparts. The finding motivates us that learning from 2D as pretraining could bring additional information which cannot be easily learned using only 3D data. Hence, we would like to raise a core problem: *how to transfer pretrained 2D network to 3D effectively without using additional labeled data*, given the difference of their data properties and the heterogeneous network structures?

Similar to the cross-modal knowledge distillation [26], we view the 2D neural network as the teacher and the 3D counterpart as the student. However, unlike the 2D images and depth maps in [26], 2D image data and 3D point clouds are not naturally aligned. It is challenging to align intermediate network representations between 2D and 3D due to the heterogeneous network structures.

Toward this goal, we propose the novel contrastive *pixel-to-point* knowledge transfer (PPKT) for 3D pretraining. The key idea is to learn the point-level features of 3D network from the corresponding pixel representations extracted from pretrained 2D networks. Despite training the 2D network beforehand, our method does not rely on additional labeled data, saving labeling efforts for 3D data. To enable the knowledge transfer process, we construct the pixel-point mappings and align pixel- and point-features with a differentiable back-projection function. To overcome the lack of pixel-level outputs of common 2D networks, *e.g.*, ResNet [27], we introduce the learnable upsampling feature projection layer (UPL), a modified version of projection layer in common contrastive learning frameworks [15], [28], which is applied on local image features and restores the spatial resolution of the feature map back to the original size (see Figure 2). Our method is able to pretrain the 3D network with the knowledge of 2D networks without strict restrictions on 2D or 3D network architectures (*e.g.*, output channel size or the output spatial resolution).

Following the pretrain-finetune protocol in [12], we show that PPKT consistently improves overall downstream performance across multiple real-world 3D tasks and datasets. Specifically, we adopt the state-of-the-art 3D network, SR-UNet [5], as the target network for pretraining and fine-tune on object detection and semantic segmentation tasks, including ScanNet [10], S3DIS [29] and SUN RGB-D [9], [30]–[32]. We achieve +3.17 mAP@0.25 improvement on ScanNet object detection and +3.12 mIoU on S3DIS semantic segmentation compared to training from scratch. We also provide an extensive ablation study to further verify the effectiveness of our proposed method.

Our contributions can be summarized as follows:

- We are the first to explore 3D pretraining by leveraging existing 2D pretrained knowledge for high-level, real-world 3D recognition tasks.
- We propose the novel contrastive pixel-to-point knowledge transfer (PPKT), enabling effective knowledge transfer from 2D to 3D as 3D pretraining.
- We show the effectiveness of our pretraining method by fine-tuning 3D models on various real-world 3D scene understanding tasks and successfully improve the overall performance compared to training from scratch.

## II. RELATED WORK

### A. 3D Deep Neural Networks

In recent years, deep neural network architectures for 3D data, *e.g.*, point clouds or meshes, have been widely investigated. For example, MVCNN [33] applies ordinary 2D convolutional neural networks (CNN) on the 2D projections of 3D objects. 3D convolutional neural networks [34] perform on the quantized volumetric grid (*i.e.*, voxels), and some specially-designed data structures and sparse convolutions [4], [5], [35] have been proposed to mitigate the high computation overhead of 3D CNN. To directly consume raw 3D point clouds, PointNet [1] leverages permutation invariant operators to handle the unordered point data. Many works improve the point-based network architecture through hierarchical aggregation [2], [36], [37], graph-based operations [38]–[41], or extending the spatial convolution on 3D point cloud [42]–[46].

On the other hand, some works design network architectures that fuse 2D image information with 3D data for 3D recognition tasks, such as 3D semantic segmentation [23], [24], 3D object detection [47]–[49], and 3D instance segmentation [50]. The advantage of fusing multi-modal data for neural networks is that networks for different modalities capture complementary information [23], [24].

### B. Self-supervised Representation Learning

The recent success of BERT [13] and pretraining in NLP have brought the interest of self-supervised representation learning into computer vision. Previous methods [51]–[56] train 2D neural networks by designing handcrafted self-supervised pretext tasks to learn informative representations. Recently, many works [15]–[22], [28] utilized contrastive learning and its variants for self-supervised representation learning, which largely improve the overall performance. They also show that models learned by self-supervised contrastive learning can be used as a good initial weight for other downstream tasks.

Some further extend the self-supervised representation learning to the 3D vision [57]–[59]. Yet, these methods take single, clean 3D objects as input, which are not applicable to complex real-world 3D data. On the other hand, Point-Contrast [12] introduces contrastive-based loss designed for point clouds for 3D pretraining, especially for 3D scene understanding tasks.

### C. Knowledge Distillation and Cross-modal Pretraining

Knowledge distillation (KD) or knowledge transfer [60]–[62] is proposed to compress a large model (teacher) into a smaller one (student) by learning the class-level soft-output of the teacher. Many works enhance KD by mimicking the teacher’s intermediate representations [63], [64], advanced objective function [65]–[69], or learnable proxy layers [70]. In addition to model compression, some recent works [71]–[73] utilize KD as a tool to increase the original performance of the network.

Knowledge distillation across modalities takes advantage of modality with rich labeled data to help the target modality

with data shortage. Gupta *et al.* [26] first propose the idea that transfers the supervision of CNN from RGB images to depth maps with unlabeled pair data. It shows that pretraining with cross-modal KD can improve the performance of the model of the target modality compared to the random initialization. Similarly, some consider distillation from RGB images to sound [74] and video [75], [76]. Note that, unlike general knowledge distillation, the distillation process here relies on paired but unlabeled data. Therefore, the cross-entropy loss that originally applies to the student and the true label cannot be used.

Despite the cross-modal knowledge distillation, many works leverage the ImageNet-pretrained CNN to initialize the neural networks on the target domain using different approaches. For example, Zhang *et al.* [77] pretrain 3D neural networks by inflating the 2D image data into 3D to build a 3D pretraining dataset; Merino *et al.* [78] transform weights of 2D convolutions into 3D convolutions as the weight initialization for the 3D neural network.

### III. LEARNING FROM 2D FOR 3D PRETRAINING

#### A. Motivation: 2D Pretraining on 3D Tasks is Effective

In the beginning, we conduct a simple pilot study showing the motivation and opportunity of pretraining deep neural networks for 3D tasks. We train a 2D semantic segmentation network to perform 3D semantic segmentation on ScanNet [10] by aggregating multi-view predictions [24]. The result is shown in Table I. The 2D network with ImageNet pretraining achieves +5.75% 2D mIoU and +4.81% 3D mIoU improvements compared to training from scratch. The result indicates (1) **pretraining effect**: with proper 3D pretraining, 3D neural networks may perform better; (2) **2D knowledge**: 2D pretraining knowledge, *e.g.*, ImageNet, may be helpful for 3D scene understanding tasks such as ScanNet semantic segmentation. Based on the observations, instead of developing a pure 3D self-supervised pretraining method, we aim to design a novel approach to transfer the 2D pretrained network knowledge into 3D as pretraining for 3D.

TABLE I  
EVALUATION OF IMAGENET PRETRAINED 2D FCN ON SCANNET 3D SEMANTIC SEGMENTATION.

Method	2D mIoU	3D mIoU
From scratch	45.38	40.46
ImageNet pretrained	51.13	45.27

#### B. Contrastive Pixel-to-point Knowledge Transfer

Assuming that a 2D neural network has been pretrained by a large-scale 2D image dataset (*e.g.*, ImageNet), we aim to learn a general initial weight for the 3D network using unlabeled datasets. Then, during the fine-tune stage, the 3D network can be fine-tuned in a supervised manner for various 3D downstream tasks, such as 3D semantic segmentation or 3D object detection.

To better exploit the 2D knowledge for 3D pretraining, we propose the novel contrastive pixel-to-point knowledge

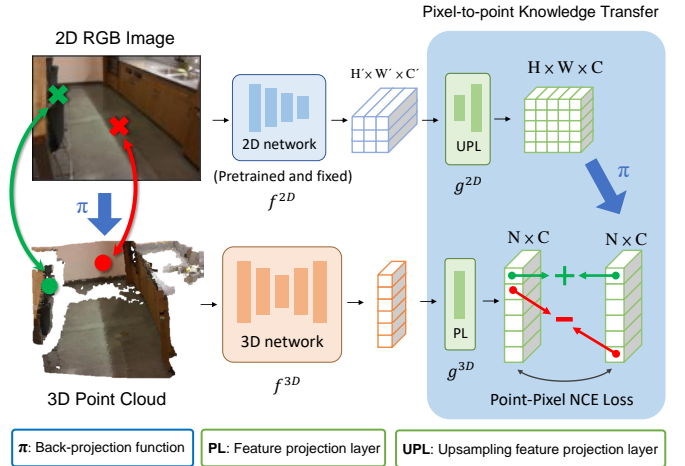


Fig. 2. **Contrastive pixel-to-point knowledge transfer (PPKT)**. PPKT transfers the 2D pretrained network knowledge into 3D from pixels to points. A back-projection is used to align corresponding pixel-level features and point-level features. To restore the granularity of low-resolution 2D feature maps, we propose the learnable upsampling feature projection layer (UPL). The details are described in Section III-B.

transfer (PPKT) from 2D to 3D. We illustrate the overview of our proposed method in Figure 2. For explanation, we divide our method into three parts: (1) the pixel-to-point design, (2) the upsampling feature projection layer, and (3) point-pixel NCE loss.

For our PPKT pretraining, we utilize a large unlabeled RGB-D image dataset to build 2D-3D data pairs. This is because unlabeled RGB-D images are easy to collect by using inexpensive RGB-D cameras, such as RealSense and Kinect. The RGB-D dataset is denoted as  $\mathcal{D} = \{(\mathbf{x}_i, \mathbf{d}_i)\}_{i=1}^{|\mathcal{D}|}$ , where  $\mathbf{x} \in \mathbb{R}^{H \times W \times 3}$  and  $\mathbf{d} \in \mathbb{R}^{H \times W}$  are the aligned RGB image and depth map.

Given the camera intrinsic parameters, we use the back-projection function to generate a single-view point cloud from an RGB-D image and construct the 2D-3D pixel-point mapping. Specifically, the function is defined as  $\pi: (\mathbf{z}, \mathbf{d}) \rightarrow (\mathbf{c}, \mathbf{f})$ , where  $\mathbf{z}$  is a 3-dimensional matrix with shape  $H \times W \times C$ , which can be an RGB image ( $C = 3$ ) or a 2D feature map ( $C$  is the feature dimension);  $\mathbf{c} \in \mathbb{R}^{N \times 3}$  is the coordinate of 3D points, and  $\mathbf{f} \in \mathbb{R}^{N \times C}$  is the point features. In other words,  $\pi$  generates a point cloud with RGB values if the input is a pair of a depth map and an RGB image. If the input is a depth map and a 2D feature map, the output point cloud has point features copied from the corresponding pixel features.

Additionally, we define the 2D and 3D neural networks. Let  $f^{2D}$  be a 2D convolutional neural network which takes an image  $\mathbf{x}$  as input and outputs a feature map with size  $H' \times W' \times C$ <sup>1</sup>. We define a 3D neural network  $f^{3D}: (\mathbf{c}, \mathbf{f}) \rightarrow (\mathbf{c}, \mathbf{f}')$  which outputs features for each point. This formulation can represent most of the common 3D network backbones, *e.g.*, SR-UNet [5] or PointNet++ [2].

1) *Knowledge transfer from pixels to points*: A naive cross-modal knowledge distillation approach is to minimize the dis-

<sup>1</sup>Without loss of generality, we ignore the final global pooling and classification layer.

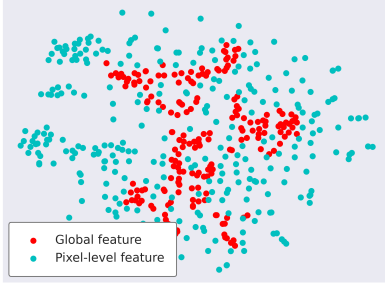


Fig. 3. **T-SNE plot of global features versus pixel-level features.** For the images in ScanNet scene0000\_00, the global features of images extracted from ImageNet pretrained ResNet are less discriminative in feature space than pixel-level features. Therefore, we believe that pixel-level features are more favorable for knowledge transfer and can preserve fine-grained pixel-level information.

tance between global features [26], or classification logits [62] of two models with different modalities. However, we found that it does not work well between 2D images and 3D point clouds in practice. PointContrast [12] argues that 3D datasets has large number of points but small number of instances (*i.e.*, scenes). Therefore, learning global representations for 3D will suffer from the limited number of instances.

In addition, we suppose that there are a few other reasons: (1) Global pooling operations cause spatial information loss. (2) For common 3D encoder-decoder network backbones, only the encoder would be pretrained in this way, and the decoder is ignored. (3) Unlike ordinary 2D datasets for self-supervised learning, RGB-D frames in indoor environments may contain similar global contexts, which are not discriminative in feature space. For example, most of the image frames contain the floor, walls, or tables, sharing similar global semantic meaning. To depict our hypothesis, Figure 3 visualizes the global features and pixel-level features encoded by ImageNet pretrained ResNet [27] from indoor scene images of ScanNet dataset [10]. The pixel-level features are more diverse in the embedding space and thus favorable for knowledge distillation. Therefore, we propose knowledge transfer between the *pixel-level* of images and the *point-level* of point clouds.

Toward this goal, we obtain the 2D and 3D feature representations encoded by the networks and align the corresponding pixels and points. Given a pair of the RGB image  $\mathbf{x}$  and the depth map  $\mathbf{d}$ , the 3D feature representation  $\mathbf{z}^{3D}$  and the pixel-to-point 2D representation  $\mathbf{z}^{2D}$  are defined as

$$\mathbf{z}^{3D} = g^{3D} \left( f^{3D}(\pi(\mathbf{x}, \mathbf{d})) \right), \quad (1)$$

$$\mathbf{z}^{2D} = \pi \left( g^{2D}(f^{2D}(\mathbf{x})), \mathbf{d} \right), \quad (2)$$

where  $g^{2D}$  and  $g^{3D}$  are learnable feature projection layers which map the feature of 2D and 3D into the same embedding space with identical dimension sizes. In practice,  $g^{2D}$  could be a  $1 \times 1$  convolution layer, and  $g^{3D}$  is a shared linear perceptron. Both  $g^{2D}$  and  $g^{3D}$  are followed with the L2 normalization. On the other hand,  $z^{2D}$  is the 2D feature representation that is back-projected into 3D space by  $\pi$ . In this way,  $z^{2D}$  and  $z^{3D}$  are well-aligned such that the 2D feature in  $i$ -th pixel  $z_i^{2D}$

and the  $i$ -th point feature  $z_i^{3D}$  are from the same coordinate in the 3D world.

2) *Upsampling feature projection layer (UPL)*: ImageNet classification pretrained network weights are commonly used in 2D computer vision since the dataset is diverse and large in scale, providing good generalizability and transferability. However, the low spatial resolution of the feature map of the classification network (*i.e.*,  $H' \ll H$  and  $W' \ll W$ ) makes it difficult for our contrastive pixel-to-point knowledge transfer.

Therefore, we introduce the upsampling feature projection layer for  $g^{2D}$  to tackle this issue. Specifically, given the feature map from the last layer of 2D CNN, we apply an  $1 \times 1$  convolution and a bilinear upsampling to the original input image resolution, inspired by the decoder head in FCN [79]. It also maps the 2D features into the same dimension as 3D. The method is simple yet effective. More importantly, it enables the flexibility to handle the spatial resolution differences and channel sizes of various 2D network architectures.

3) *Point-pixel NCE loss*: As the learning objective, we minimize the relative distance between the corresponding pixel and point representation through point-pixel NCE loss (PPNCE), a modified version of InfoNCE loss [21] for contrastive learning, which is defined as

$$\mathcal{L}_{\text{PPNCE}} = - \sum_{i=1}^N \log \frac{\exp(\mathbf{z}_i^{3D} \cdot \mathbf{z}_i^{2D} / \tau)}{\sum_{j=1}^N \exp(\mathbf{z}_i^{3D} \cdot \mathbf{z}_j^{2D} / \tau)} \quad (3)$$

where  $\tau$  is the temperature hyper-parameter, the  $\cdot$  notation here is the dot-product, and  $N$  is the total number of points. The physical meaning of the loss function is to form a feature space by attracting a 3D point feature and its corresponding 2D pixel feature while separating the 3D feature from other 2D features at the same time. In other words, if a pixel and a point share the same coordinate in the 3D world, they are positive pairs; otherwise, they are negative pairs. For empirical memory concern, we sub-sample a fixed number of points and pixels for the loss calculation.

Note that most existing contrastive learning methods apply linear or non-linear feature projection layers on the *global* features by multi-layer perceptrons [15], [28], [69]. In contrast, our 3D feature projection layer  $g^{3D}$  is applied on 3D point-level feature maps, and the 2D upsampling projection layer  $g^{2D}$  is applied on 2D high-level but low-resolution feature maps. For simplicity, we do not include memory bank [28] due to the large number of pixels and points.

4) *Discussion*: Our problem formulation is similar to the cross-modal knowledge distillation [26], considering that the 2D network is the teacher and the 3D network is the student. However, the key difference is that that RGB images and depth maps in [26] are well-aligned while 2D images and 3D point cloud are not, and the networks for 2D and 3D are heterogeneous.

If we consider the back-projected pixel-level features as pseudo 3D points, our loss function is similar to PointInfoNCE [12]. We both apply contrastive loss on point-level (or pixel-level) instead of global instance level, which is commonly presented in 2D contrastive learning. However, our PPNCE is applied across 2D and 3D features encoded by

two *different networks* from the same data pair. In contrast, PointInfoNCE is applied across features of two different point cloud samples extracted by the *same 3D network*. Additionally, our motivation is different. We propose using contrastive loss to minimize the relative distance between the point and the pixel representation to transfer the 2D knowledge to 3D as pretraining.

#### IV. EXPERIMENT

In this section, we study the effectiveness of our proposed 3D pretraining method. The experiment focuses on the ability to transfer the 3D network pretrained by our method to various downstream tasks and whether it can improve the performance compared to training from scratch. Specifically, the evaluation is divided into three steps: (1) Given a pretrained 2D neural network, we pretrain the 3D neural networks by PPKT with an unlabeled RGB-D dataset. (2) We fine-tune the model for the target downstream tasks in a supervised manner, including 3D semantic segmentation and 3D object detection. (3) We evaluate the fine-tune performance on the testing data. In the following, we will describe the details and results.

##### A. Experimental Setup of 3D Pretraining

1) *Network architectures*: Our PPKT requires a pretrained 2D neural network as the teacher. Therefore, we choose the most widely-used ResNet [27] pretrained on ImageNet classification as our 2D backbone. For the 3D network, following [12], we adopt the Sparse Residual 3D U-Net 34 (SR-UNet34) [4], [5] since it achieves state-of-the-art performance on multiple 3D tasks. It contains 34 layers of 3D sparse convolution layers with the encoder-decoder design and skip connections. SR-UNet is innately suitable for the 3D semantic segmentation task since it generates per-point outputs. Following [12], it can also perform 3D object detection by attaching VoteNet [80] modules.

2) *Datasets*: For pretraining, we use the raw RGB-D images in ScanNet dataset [10], collected by hand-held lightweight depth sensors, since it is currently the largest available real-world dataset of its kind. ScanNet contains 1513 indoor scans for 707 distinct spaces. We sub-sample every 25 frames from the sequential RGB-D data, resulting in about 100k frames in total.

3) *Baselines*: We consider different pretraining approaches for the 3D neural network as baselines. In particular, we compared our method with PointContrast [12] using the officially-released pretrained weight. Additionally, to prove the effectiveness of our design, we build other naive 2D-3D knowledge transfer methods for comparison. Global knowledge distillation (Global KD) represents the method we modified from [62], considering the SR-UNet *encoder* as the student and 2D CNN as the teacher. Precisely, we extract the encoder part from SR-UNet and attach a mean pooling layer and a classifier where the output number of classes matched with the ImageNet supervised pretrained network (*i.e.*, output 1000 classes). We minimize the KL-divergence between 2D and 3D logits. Even though the dataset we used is not from ImageNet, we force the 2D classifier to output “dark” class information

as the learning target for the 3D network. Note that since the dataset has no label, the classification loss between student and true label is ignored. In other words, the student (SR-UNet encoder) is purely mimicking the teacher’s output.

CRD [81] follows the similar settings with Global KD but minimizes the contrastive-based loss function instead of traditional KD loss. We also compared with [26] with slight modifications to adapt to our 2D-3D settings, which is minimizing the L2 distance between 2D and 3D global features. Note that for Global KD, CRD, and [26] baselines, only the 3D encoder is pretrained. We provide the summary of baselines in Table II.

TABLE II  
THE SUMMARY OF THE 3D PRETRAINING BASELINES

Method	Objective	Pretrained 3D network	Loss function
Global KD	2D $\rightarrow$ 3D	encoder	Global KL-div
CRD [69]	2D $\rightarrow$ 3D	encoder	Global contrastive
Gupta <i>et al.</i> [26]	2D $\rightarrow$ 3D	encoder	Global L2
PointContrast [12]	3D $\leftrightarrow$ 3D	encoder-decoder	Local contrastive
PPKT (ours)	2D $\rightarrow$ 3D	encoder-decoder	Local contrastive

4) *Training details of PPKT*: We apply the upsampling feature projection layer on the 2D ResNet50 layer4 output. As for 3D, a feature projection layer is used to project the last layer feature of SR-UNet. The projected feature dimension 128. The temperature of NCE loss is 0.04. The voxel size is set as 2.5cm, and the input image size is [480, 640]. We use momentum SGD with learning rate 0.5 and weight decay 1e-4. The exponential learning rate scheduler is used. We apply 2D augmentations, including horizontal flip and random resize, and 3D augmentations, including scaling, rotation, and elastic distortion. We pretrain the 3D network for 60k iterations using one V100 GPU with batch size 24. We use the same PPKT pretrained 3D network as the initial weight for all the downstream tasks and datasets during fine-tune stage.

##### B. Fine-tune on S3DIS Semantic Segmentation

1) *Setup*: Stanford Large-Scale 3D Indoor Spaces dataset (S3DIS) [29] contains 6 large buildings, nearly 250 rooms, and semantic labels of 13 categories. For evaluation, we follow the most common setup which takes area 5 for validation. For training, we use 5cm voxel size and follow most of the details in [12]. We use SGD+momentum with learning rate 0.1 and polynomial learning rate scheduler. We apply common 3D data augmentations during fine-tuning, including scaling, rotation, chromatic distortion, elastic distortion, translation, and point dropout. We use batch size 32 and one V100 GPU training for 15k iterations. Note that we apply the same fine-tune details for all the baselines’ and our pretrained 3D models, including the random seed. The evaluation metrics are the mean class accuracy and mean class IoU. We report the final validation performance.

2) *Result*: The result of S3DIS semantic segmentation is shown in Table III. Compared to training from scratch, our proposed contrastive pixel-to-point knowledge transfer pretraining brings significant improvements (+3.34% mIoU). In contrast, the performances of global learning from 2D baselines (Global

TABLE III  
FINE-TUNE RESULT ON S3DIS SEMANTIC SEGMENTATION.

Method	mean Acc	mean IoU
From scratch	73.24	65.16
Global KD	72.65	66.56
Gupta <i>et al.</i> [26]	72.11	64.39
CRD [69]	72.70	65.65
PointContrast [12]	73.97	66.86
PPKT (ours)	<b>75.19</b>	<b>68.28</b>

TABLE V  
FINE-TUNE RESULT ON SCANNET SEMANTIC SEGMENTATION AND OBJECT DETECTION. SEE SECTION IV-D AND FIGURE 4 FOR MORE DETAIL ON SEMANTIC SEGMENTATION RESULT.

Method	Semantic segmentation		Object detection	
	mean Acc	mean IoU	mAP@0.25	mAP@0.5
From scratch	88.57	69.49	56.50	34.54
Global KD	<b>88.63</b>	<b>70.35</b>	57.50	34.81
Gupta <i>et al.</i> [26]	88.40	68.71	56.74	36.27
CRD [69]	88.08	68.53	56.82	36.75
PointContrast [12]	<b>88.63</b>	69.22	58.30	36.26
PPKT (ours)	88.53	69.56	<b>59.67</b>	<b>38.90</b>

KD, CRD, Gupta *et al.*) are similar to training from scratch, which indicate that the pretraining effects of these baselines are limited. The comparison suggests that (1) pretraining the encoder-decoder is helpful, and (2) our pixel-to-point design is important to effectively transfer 2D knowledge since those baselines and our method all use the same ImageNet-pretrained 2D teacher network.

### C. Fine-tune on SUN RGB-D Object Detection

1) *Setup*: SUN RGB-D dataset [9] comprises about 10,000 RGB-D images and is annotated with 60k 3D oriented bounding boxes of 37 object classes. The RGB-D images are back-projected into 3D point clouds. We use the official train/val split and train with the ten most common object classes. For training details, we use 64 for batch size and 5cm voxel size. We use Adam optimizer with 0.001 learning rate training for 180 epochs on one V100 GPU. The learning rate is decreased 10x after 80 and 120 epochs. For data augmentations, we adopt random rotation, scaling, and flipping. The evaluation metric is the mean AP considering two 3D IoU threshold, 0.25 and 0.5. We report the final validation performance.

2) *Result*: The result of our pretrained model against training from scratch is summarized in Table IV. 3D object detection requires high-level semantic understanding for object classification and localization. Our proposed contrastive pixel-to-point knowledge transfer achieves significant improvement compared to training from scratch (+2.28% mAP@0.25). The performance improvement is consistent with the result in the S3DIS semantic segmentation, showing the generalization ability of our pretrained weights.

### D. Fine-tune on ScanNet Semantic Segmentation and Object Detection

1) *Setup*: ScanNet [10] dataset contains 1201 scans in training set and 312 in validation set. For semantic segmentation,

TABLE IV  
FINE-TUNE RESULT ON SUN RGB-D 3D OBJECT DETECTION.

Method	mAP@0.25	mAP@0.5
From scratch	55.21	32.81
Global KD	56.10	33.58
Gupta <i>et al.</i> [26]	54.42	31.12
CRD [69]	55.86	<b>34.30</b>
PointContrast [12]	56.14	32.70
PPKT (ours)	<b>57.26</b>	33.92

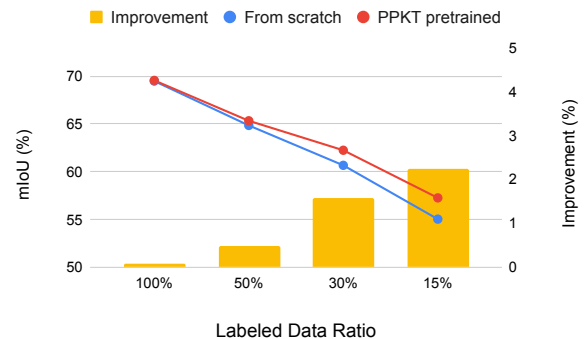


Fig. 4. **Limited labeled data fine-tuning on ScanNet semantic segmentation.** We sub-sample the labeled scenes in the ScanNet dataset into 50%, 30%, and 15%. With less labeled data available, the gap between our PPKT pretraining and training from scratch becomes larger.

we use the v2 label set, which has 20 semantic classes and evaluate the performance on vertex points. We use 2cm voxel size. We split the origin training set into train/val 949/525 scenes. We save the best validation score and test on the original validation set. We use SGD+momentum with learning rate 0.1 and polynomial learning rate scheduler. The batch size is 12 for a single GPU. We use 4 V100 GPUs training for 15k iterations. We use the same augmentations as in S3DIS. During testing, the points are assigned to the predicted class of the nearest voxel center.

For object detection, ScanNet contains 18 object classes for instance segmentation labeled on mesh data. We follow the preprocessing of [12], [80], generating 3D axis-aligned bounding box. Compared to SUN RGB-D, ScanNet consists of reconstructed 3D scans, which are larger and more complete. We set 2.5cm for voxel size and follow the training details in [12].

2) *Result*: The semantic segmentation and object detection results are shown in Table V. For semantic segmentation, the pretraining has little performance improvement against training from scratch. Since the supervised fine-tune dataset is the same as our pretraining dataset, we suggest that self-supervised pretraining only accelerates the training process but hardly brings performance improvements. For verification, we experiment reducing the number of labeled data in ScanNet for fine-tuning gradually. We randomly sample 50%, 30%, 15% of the labeled scenes in the dataset for fine-tuning, and the result is presented in Figure 4. Although there is no pretraining gain using 100% labeled data during fine-tuning, the performance gap between pretraining and training from scratch becomes larger when the data size is smaller (2.23% mIoU difference

TABLE VI  
**3D BACKBONE ABLATION STUDY ON S3DIS.** THE MODELS WITH LARGER CAPACITY BENEFIT MORE FROM PRETRAINING WITH RICH UNLABELED DATA.

Method	mean Acc	mean IoU
SR-UNet18	71.67	64.67
SR-UNet18 + PPKT	73.67 (+2.0)	66.40 (+1.73)
SR-UNet34	73.24	65.16
SR-UNet34 + PPKT	<b>75.19</b> (+1.95)	<b>68.28</b> (+3.12)

TABLE VII  
**POINT-PIXEL LOSS ABLATION STUDY ON SUN RGB-D OBJECT DETECTION.** PPNCE LOSS IS PREFERRED OVER PPKD. SEE SECTION IV-E2 FOR MORE DETAIL.

Loss	2D Dataset	2D Network	mAP@0.25
From scratch	-	-	55.21
PPKD loss	ADE20k	ResNet-FCN	56.07
PPNCE loss	ADE20k	ResNet-FCN	<b>58.03</b>
PPNCE loss	ImageNet	ResNet	57.26

for 15% labeled data). Our limited labeled data fine-tune result also matches the findings in previous works [82], [83], which suggest that self-supervised pretraining methods benefit more when the size of labeled data is smaller in the downstream supervised task.

For object detection, unlike the semantic segmentation result, our contrastive pixel-to-point knowledge transfer increases the performance by a large margin (+3.17% mAP@0.25 and +4.36% mAP@0.5) even if the pretraining dataset and fine-tune dataset are the same. The improvements are consistent with the results in SUN RGB-D object detection. This may suggest that 3D object detection tasks benefit more from the high-level semantics learned from the 2D pretrained knowledge.

### E. Ablation Study

1) *Backbone network size:* Previous works [82], [83] have shown that larger or deeper 2D networks will benefit more from self-supervised pretraining. Therefore, we would like to study the effect of our PPKT pretraining for different 3D network sizes. We provide the ablation study on S3DIS in Table VI. SR-UNet18 has about half the size in terms of network parameters compared to SR-UNet34. The result shows that our PPKT pretraining on larger models has more performance improvement, which is similar to the finding in the previous works. It is also worth noticing that our PPKT pretraining on SR-UNet18 could achieve the performance of SR-UNet34 training from scratch. In other words, a good pretraining can make up the network backbone size limitation.

2) *Point-pixel loss functions and datasets:* We study the loss function in our pixel-to-point knowledge transfer by replacing PPNCE loss with the ordinary knowledge distillation loss [62] applied on points and pixels (PPKD). However, ImageNet pretrained ResNet does not have pixel-wise class-level predictions. To achieve this, we train a 2D ResNet-FCN [79] with ADE20k semantic segmentation dataset [84] as the 2D teacher network. We evaluate the fine-tune performance on SUN RGB-D object detection in Table VII. The result

TABLE VIII  
**PPKT WITH SELF-SUPERVISED PRETRAINED 2D NETWORK AS TEACHER ON 3D OBJECT DETECTION.** SEE SECTION IV-E3 FOR MORE DETAIL.

Method	mAP@0.25	
	ScanNet	SUNRGBD
From scratch	56.50	55.21
PPKT (ImageNet super.)	59.67	<b>57.26</b>
PPKT (ImageNet MoCo [15])	<b>59.69</b>	57.17

shows that pretraining with both loss functions are better compared to training from scratch, and PPNCE is better than PPKD (+2.03% mAP@0.25). This is because, in contrast to traditional KD loss, which treats each output independently, the contrastive loss is better to transfer the knowledge in structurally due to the large numbers of negative examples [69].

On the other hand, ADE20k PPNCE performs better than the ImageNet PPNCE. Nevertheless, we believe that 2D teacher network architectures without decoder (*e.g.*, FCN) combined with the UPL are the better choices since FCN-like structure requires semantic segmentation dataset to pretrain. In contrast, our default setup has more flexibility and weaker assumption on 2D network architectures.

3) *Learning from 2D self-supervised pretrained teacher network:* We further show that our PPKT is not limited to 2D teacher networks that are pretrained by supervised learning (*e.g.*, ImageNet classification). It can also take advantage of 2D self-supervised pretrained model as teacher. Here, we use a 2D ResNet50, which is self-supervised pretrained by MoCo [15] beforehand, as teacher for PPKT and compared to our default settings, where ImageNet supervised teacher is used.

We show the result in Table VIII. In our experiment, the 3D model learned from MoCo-pretrained 2D teacher shows comparable fine-tune performance with the 3D model learned from the supervised ImageNet classification teacher. We believe that the performance could be further improved if the 2D self-supervised teacher is pretrained with an unlabeled dataset larger than ImageNet, which is the strength of self-supervised learning.

### F. Visualization

We provide the visualization of the learned features of PPKT *without fine-tuning* in Figure 5. We extract the point-level features from the last layer of SR-UNet (before the segmentation head) of the 3D scan scene0000\_00 in the ScanNet dataset and visualize them with T-SNE. For fair comparison, except for the network weights, all the other settings remain identical. Remarkably, without any labeled data during pretraining, our pretrained network is able to encode semantic meaningful point embedding by exploiting the rich 2D pretrained knowledge. This shows that learning from 2D with PPKT is a promising approach to provide pretraining weights for 3D neural networks, especially for those tasks that require high-level semantic understanding.

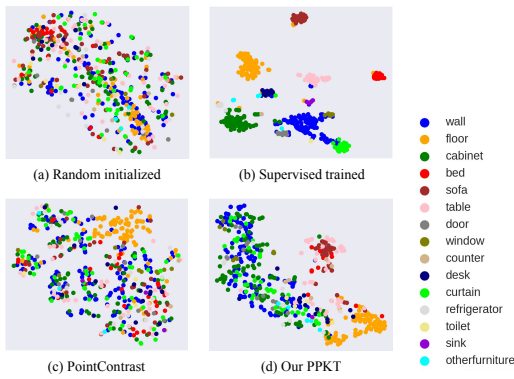


Fig. 5. **T-SNE visualization of point-level features in ScanNet.** We visualize the last-layer point features of a 3D scene using different 3D network weights. The feature points are colored with segmentation class labels. Without any 3D labeled data, our method shows the high-level semantic understanding ability by learning from 2D rich information.

## V. CONCLUSION

In this work, we explore a new 3D pretraining approach by learning from 2D pretrained networks. We present the contrastive pixel-to-point knowledge transfer (PPKT) to exploit the 2D knowledge effectively. We show that combining the pixel-to-point design and the contrastive loss helps learn good initial weights for 3D models with large unlabeled RGB-D data. We also demonstrate that 3D pretraining through PPKT is more effective when the network size is larger, or the fine-tune labeled dataset is limited. Moreover, our method is complementary to PointContrast [12]. We expect that our idea of learning from 2D and empirical findings could inspire future works to consider 2D network knowledge when developing self-supervised 3D algorithms.

## APPENDIX EXPERIMENT RESULT DETAILS

We provide per-class performance for S3DIS in Table IX, SUN RGB-D in Table X, and ScanNet in Table XI.

## REFERENCES

- [1] C. R. Qi, H. Su, K. Mo, and L. J. Guibas, "Pointnet: Deep learning on point sets for 3d classification and segmentation," in *Proceedings of the IEEE conference on computer vision and pattern recognition*, 2017, pp. 652–660.
- [2] C. R. Qi, L. Yi, H. Su, and L. J. Guibas, "Pointnet++: Deep hierarchical feature learning on point sets in a metric space," *arXiv preprint arXiv:1706.02413*, 2017.
- [3] Y. Wang, Y. Sun, Z. Liu, S. E. Sarma, M. M. Bronstein, and J. M. Solomon, "Dynamic graph cnn for learning on point clouds," *Acm Transactions On Graphics (tog)*, vol. 38, no. 5, pp. 1–12, 2019.
- [4] B. Graham, M. Engelcke, and L. Van Der Maaten, "3d semantic segmentation with submanifold sparse convolutional networks," in *Proceedings of the IEEE conference on computer vision and pattern recognition*, 2018, pp. 9224–9232.
- [5] C. Choy, J. Gwak, and S. Savarese, "4d spatio-temporal convnets: Minkowski convolutional neural networks," in *Proceedings of the IEEE/CVF Conference on Computer Vision and Pattern Recognition*, 2019, pp. 3075–3084.
- [6] Z. Liu, H. Tang, Y. Lin, and S. Han, "Point-voxel cnn for efficient 3d deep learning," *arXiv preprint arXiv:1907.03739*, 2019.
- [7] H. Tang, Z. Liu, S. Zhao, Y. Lin, J. Lin, H. Wang, and S. Han, "Searching efficient 3d architectures with sparse point-voxel convolution," in *European Conference on Computer Vision*. Springer, 2020, pp. 685–702.
- [8] J. Deng, W. Dong, R. Socher, L.-J. Li, K. Li, and L. Fei-Fei, "Imagenet: A large-scale hierarchical image database," in *2009 IEEE conference on computer vision and pattern recognition*. Ieee, 2009, pp. 248–255.
- [9] S. Song, S. P. Lichtenberg, and J. Xiao, "Sun rgb-d: A rgb-d scene understanding benchmark suite," in *Proceedings of the IEEE conference on computer vision and pattern recognition*, 2015, pp. 567–576.
- [10] A. Dai, A. X. Chang, M. Savva, M. Halber, T. Funkhouser, and M. Nießner, "Scannet: Richly-annotated 3d reconstructions of indoor scenes," in *Proceedings of the IEEE Conference on Computer Vision and Pattern Recognition*, 2017, pp. 5828–5839.
- [11] A. Geiger, P. Lenz, C. Stiller, and R. Urtasun, "Vision meets robotics: The kitti dataset," *The International Journal of Robotics Research*, vol. 32, no. 11, pp. 1231–1237, 2013.
- [12] S. Xie, J. Gu, D. Guo, C. R. Qi, L. Guibas, and O. Litany, "Pointcontrast: Unsupervised pre-training for 3d point cloud understanding," in *European Conference on Computer Vision*. Springer, 2020, pp. 574–591.
- [13] J. Devlin, M.-W. Chang, K. Lee, and K. Toutanova, "Bert: Pre-training of deep bidirectional transformers for language understanding," *arXiv preprint arXiv:1810.04805*, 2018.
- [14] A. Radford, J. Wu, R. Child, D. Luan, D. Amodei, and I. Sutskever, "Language models are unsupervised multitask learners," *OpenAI blog*, vol. 1, no. 8, p. 9, 2019.
- [15] K. He, H. Fan, Y. Wu, S. Xie, and R. Girshick, "Momentum contrast for unsupervised visual representation learning," in *Proceedings of the IEEE/CVF Conference on Computer Vision and Pattern Recognition*, 2020, pp. 9729–9738.
- [16] P. Bachman, R. D. Hjelm, and W. Buchwalter, "Learning representations by maximizing mutual information across views," in *Advances in Neural Information Processing Systems*, 2019, pp. 15 535–15 545.
- [17] J.-B. Grill, F. Strub, F. Alché, C. Tallec, P. H. Richemond, E. Buchatskaya, C. Doersch, B. A. Pires, Z. D. Guo, M. G. Azar *et al.*, "Bootstrap your own latent: A new approach to self-supervised learning," *arXiv preprint arXiv:2006.07733*, 2020.
- [18] O. Henaff, "Data-efficient image recognition with contrastive predictive coding," in *International Conference on Machine Learning*. PMLR, 2020, pp. 4182–4192.
- [19] R. D. Hjelm, A. Fedorov, S. Lavoie-Marchildon, K. Grewal, P. Bachman, A. Trischler, and Y. Bengio, "Learning deep representations by mutual information estimation and maximization," *arXiv preprint arXiv:1808.06670*, 2018.
- [20] I. Misra and L. v. d. Maaten, "Self-supervised learning of pretext-invariant representations," in *Proceedings of the IEEE/CVF Conference on Computer Vision and Pattern Recognition*, 2020, pp. 6707–6717.
- [21] A. v. d. Oord, Y. Li, and O. Vinyals, "Representation learning with contrastive predictive coding," *arXiv preprint arXiv:1807.03748*, 2018.
- [22] Z. Wu, Y. Xiong, S. X. Yu, and D. Lin, "Unsupervised feature learning via non-parametric instance discrimination," in *Proceedings of the IEEE Conference on Computer Vision and Pattern Recognition*, 2018, pp. 3733–3742.
- [23] A. Dai and M. Nießner, "3dmv: Joint 3d-multi-view prediction for 3d semantic scene segmentation," in *Proceedings of the European Conference on Computer Vision (ECCV)*, 2018, pp. 452–468.
- [24] H.-Y. Chiang, Y.-L. Lin, Y.-C. Liu, and W. H. Hsu, "A unified point-based framework for 3d segmentation," in *2019 International Conference on 3D Vision (3DV)*. IEEE, 2019, pp. 155–163.
- [25] A. Kundu, X. Yin, A. Fathi, D. Ross, B. Brewington, T. Funkhouser, and C. Pantofaru, "Virtual multi-view fusion for 3d semantic segmentation," in *European Conference on Computer Vision*. Springer, 2020, pp. 518–535.
- [26] S. Gupta, J. Hoffman, and J. Malik, "Cross modal distillation for supervision transfer," in *Proceedings of the IEEE conference on computer vision and pattern recognition*, 2016, pp. 2827–2836.
- [27] K. He, X. Zhang, S. Ren, and J. Sun, "Deep residual learning for image recognition," in *Proceedings of the IEEE conference on computer vision and pattern recognition*, 2016, pp. 770–778.
- [28] T. Chen, S. Kornblith, M. Norouzi, and G. Hinton, "A simple framework for contrastive learning of visual representations," *arXiv preprint arXiv:2002.05709*, 2020.
- [29] I. Armeni, O. Sener, A. R. Zamir, H. Jiang, I. Brilakis, M. Fischer, and S. Savarese, "3d semantic parsing of large-scale indoor spaces," in *Proceedings of the IEEE Conference on Computer Vision and Pattern Recognition*, 2016, pp. 1534–1543.



TABLE IX  
PER-CLASS IOU ON S3DIS SEMANTIC SEGMENTATION.

Method	clutter	beam	board	book	ceiling	chair	column	door	floor	sofa	table	wall	window	mIoU	mAcc
From scratch	56.66	<b>0.03</b>	72.83	68.68	92.78	89.17	31.49	68.03	98.07	58.64	76.49	82.83	51.43	65.16	73.24
PointContrast	<b>62.01</b>	0.00	74.39	<b>74.07</b>	<b>94.67</b>	90.18	<b>37.35</b>	70.33	<b>98.54</b>	53.35	78.80	<b>84.45</b>	51.02	66.86	73.97
PPKT (ours)	57.15	0.00	<b>78.05</b>	73.26	93.05	<b>91.00</b>	33.31	<b>77.11</b>	98.44	<b>70.46</b>	<b>79.77</b>	83.67	<b>52.25</b>	<b>68.27</b>	<b>75.19</b>

TABLE X  
PER-CLASS AP UNDER IOU 0.5 ON SUN RGB-D OBJECT DETECTION.

Method	bed	table	sofa	chair	toilet	desk	dress	night	book	bath	mAP
From scratch	47.35	<b>18.58</b>	47.96	52.23	<b>61.74</b>	5.31	<b>15.65</b>	33.16	5.69	<b>40.44</b>	32.81
PointContrast	49.95	18.38	48.52	<b>53.84</b>	53.69	5.61	14.68	36.87	7.89	37.58	32.70
PPKT (ours)	<b>52.10</b>	17.61	<b>50.34</b>	52.31	58.05	<b>6.20</b>	12.98	<b>43.72</b>	<b>9.36</b>	36.55	<b>33.92</b>

TABLE XI  
PER-CLASS AP UNDER IOU 0.5 ON SCANNET OBJECT DETECTION.

Method	cabinet	bed	chair	sofa	table	door	wind	book	pic	cntr	desk	curtn	refrig	shower	toilet	sink	bath	garbg	mAP
From scratch	10.61	68.40	64.86	53.54	37.69	20.64	9.80	30.08	0.64	13.92	36.63	24.70	<b>31.32</b>	10.57	83.49	21.66	83.39	19.73	34.54
PointContrast	<b>12.41</b>	67.22	70.06	<b>57.91</b>	<b>46.54</b>	22.72	<b>11.59</b>	37.12	0.30	10.10	36.35	<b>25.47</b>	27.30	21.64	84.96	<b>23.84</b>	75.30	21.84	36.26
PPKT (ours)	7.95	<b>70.25</b>	<b>72.56</b>	57.06	40.31	<b>23.26</b>	11.40	<b>45.26</b>	<b>3.47</b>	<b>18.80</b>	<b>38.05</b>	25.10	31.26	<b>35.50</b>	<b>86.68</b>	18.11	<b>87.09</b>	<b>28.07</b>	<b>38.90</b>

- [30] N. Silberman, D. Hoiem, P. Kohli, and R. Fergus, "Indoor segmentation and support inference from rgb-d images," in *European conference on computer vision*. Springer, 2012, pp. 746–760.
- [31] A. Janoch, S. Karayev, Y. Jia, J. T. Barron, M. Fritz, K. Saenko, and T. Darrell, "A category-level 3d object dataset: Putting the kinect to work," in *Consumer depth cameras for computer vision*. Springer, 2013, pp. 141–165.
- [32] J. Xiao, A. Owens, and A. Torralba, "Sun3d: A database of big spaces reconstructed using sfm and object labels," in *Proceedings of the IEEE international conference on computer vision*, 2013, pp. 1625–1632.
- [33] H. Su, S. Maji, E. Kalogerakis, and E. Learned-Miller, "Multi-view convolutional neural networks for 3d shape recognition," in *Proceedings of the IEEE international conference on computer vision*, 2015, pp. 945–953.
- [34] D. Maturana and S. Scherer, "Voxnet: A 3d convolutional neural network for real-time object recognition," in *2015 IEEE/RSJ International Conference on Intelligent Robots and Systems (IROS)*. IEEE, 2015, pp. 922–928.
- [35] G. Riegler, A. Osman Ulusoy, and A. Geiger, "Octnet: Learning deep 3d representations at high resolutions," in *Proceedings of the IEEE Conference on Computer Vision and Pattern Recognition*, 2017, pp. 3577–3586.
- [36] R. Klokov and V. Lempitsky, "Escape from cells: Deep kd-networks for the recognition of 3d point cloud models," in *Proceedings of the IEEE International Conference on Computer Vision*, 2017, pp. 863–872.
- [37] W. Zeng and T. Gevers, "3dcontextnet: Kd tree guided hierarchical learning of point clouds using local and global contextual cues," in *Proceedings of the European Conference on Computer Vision (ECCV) Workshops*, 2018, pp. 0–0.
- [38] S. Xie, S. Liu, Z. Chen, and Z. Tu, "Attentional shapecontextnet for point cloud recognition," in *Proceedings of the IEEE Conference on Computer Vision and Pattern Recognition*, 2018, pp. 4606–4615.
- [39] N. Verma, E. Boyer, and J. Verbeek, "Feastnet: Feature-steered graph convolutions for 3d shape analysis," in *Proceedings of the IEEE conference on computer vision and pattern recognition*, 2018, pp. 2598–2606.
- [40] Y. Shen, C. Feng, Y. Yang, and D. Tian, "Mining point cloud local structures by kernel correlation and graph pooling," in *Proceedings of the IEEE conference on computer vision and pattern recognition*, 2018, pp. 4548–4557.
- [41] C. Chen, S. Qian, Q. Fang, and C. Xu, "Hapgn: Hierarchical attentive pooling graph network for point cloud segmentation," *IEEE Transactions on Multimedia*, pp. 1–1, 2020.
- [42] B.-S. Hua, M.-K. Tran, and S.-K. Yeung, "Pointwise convolutional neural networks," in *Proceedings of the IEEE Conference on Computer Vision and Pattern Recognition*, 2018, pp. 984–993.
- [43] Y. Xu, T. Fan, M. Xu, L. Zeng, and Y. Qiao, "Spidernn: Deep learning on point sets with parameterized convolutional filters," in *Proceedings of the European Conference on Computer Vision (ECCV)*, 2018, pp. 87–102.
- [44] Y. Li, R. Bu, M. Sun, W. Wu, X. Di, and B. Chen, "Pointcnn: Convolution on x-transformed points," in *Advances in neural information processing systems*, 2018, pp. 820–830.
- [45] H. Su, V. Jampani, D. Sun, S. Maji, E. Kalogerakis, M.-H. Yang, and J. Kautz, "Splatnet: Sparse lattice networks for point cloud processing," in *Proceedings of the IEEE Conference on Computer Vision and Pattern Recognition*, 2018, pp. 2530–2539.
- [46] H. Thomas, C. R. Qi, J.-E. Deschard, B. Marcotegui, F. Goulette, and L. J. Guibas, "Kpconv: Flexible and deformable convolution for point clouds," in *Proceedings of the IEEE International Conference on Computer Vision*, 2019, pp. 6411–6420.
- [47] X. Chen, H. Ma, J. Wan, B. Li, and T. Xia, "Multi-view 3d object detection network for autonomous driving," in *Proceedings of the IEEE conference on Computer Vision and Pattern Recognition*, 2017, pp. 1907–1915.
- [48] J. Ku, M. Mozifian, J. Lee, A. Harakeh, and S. L. Waslander, "Joint 3d proposal generation and object detection from view aggregation," in *2018 IEEE/RSJ International Conference on Intelligent Robots and Systems (IROS)*. IEEE, 2018, pp. 1–8.
- [49] C. R. Qi, X. Chen, O. Litany, and L. J. Guibas, "Imvotenet: Boosting 3d object detection in point clouds with image votes," in *Proceedings of the IEEE/CVF conference on computer vision and pattern recognition*, 2020, pp. 4404–4413.
- [50] J. Hou, A. Dai, and M. Nießner, "3d-sis: 3d semantic instance segmentation of rgb-d scans," in *Proceedings of the IEEE/CVF Conference on Computer Vision and Pattern Recognition*, 2019, pp. 4421–4430.
- [51] R. Zhang, P. Isola, and A. A. Efros, "Colorful image colorization," in *European conference on computer vision*. Springer, 2016, pp. 649–666.
- [52] —, "Split-brain autoencoders: Unsupervised learning by cross-channel prediction," in *Proceedings of the IEEE Conference on Computer Vision and Pattern Recognition*, 2017, pp. 1058–1067.
- [53] D. Pathak, P. Krahenbuhl, J. Donahue, T. Darrell, and A. A. Efros, "Context encoders: Feature learning by inpainting," in *Proceedings of the IEEE conference on computer vision and pattern recognition*, 2016, pp. 2536–2544.
- [54] C. Doersch, A. Gupta, and A. A. Efros, "Unsupervised visual representation learning by context prediction," in *Proceedings of the IEEE international conference on computer vision*, 2015, pp. 1422–1430.
- [55] M. Noroozi and P. Favaro, "Unsupervised learning of visual representations by solving jigsaw puzzles," in *European Conference on Computer Vision*. Springer, 2016, pp. 69–84.
- [56] S. Gidaris, P. Singh, and N. Komodakis, "Unsupervised representation learning by predicting image rotations," *arXiv preprint arXiv:1803.07728*, 2018.
- [57] J. Sauder and B. Sievers, "Self-supervised deep learning on point clouds

- by reconstructing space,” in *Advances in Neural Information Processing Systems*, 2019, pp. 12 962–12 972.
- [58] Y. Rao, J. Lu, and J. Zhou, “Global-local bidirectional reasoning for unsupervised representation learning of 3d point clouds,” in *Proceedings of the IEEE/CVF Conference on Computer Vision and Pattern Recognition*, 2020, pp. 5376–5385.
- [59] K. Hassani and M. Haley, “Unsupervised multi-task feature learning on point clouds,” in *Proceedings of the IEEE International Conference on Computer Vision*, 2019, pp. 8160–8171.
- [60] C. Buciluă, R. Caruana, and A. Niculescu-Mizil, “Model compression,” in *Proceedings of the 12th ACM SIGKDD international conference on Knowledge discovery and data mining*, 2006, pp. 535–541.
- [61] J. Li, R. Zhao, J.-T. Huang, and Y. Gong, “Learning small-size dnn with output-distribution-based criteria,” in *Fifteenth annual conference of the international speech communication association*, 2014.
- [62] G. Hinton, O. Vinyals, and J. Dean, “Distilling the knowledge in a neural network,” *arXiv preprint arXiv:1503.02531*, 2015.
- [63] A. Romero, N. Ballas, S. E. Kahou, A. Chassang, C. Gatta, and Y. Bengio, “Fitnets: Hints for thin deep nets,” *arXiv preprint arXiv:1412.6550*, 2014.
- [64] S. Zagoruyko and N. Komodakis, “Paying more attention to attention: Improving the performance of convolutional neural networks via attention transfer,” *arXiv preprint arXiv:1612.03928*, 2016.
- [65] Z. Huang and N. Wang, “Like what you like: Knowledge distill via neuron selectivity transfer,” *arXiv preprint arXiv:1707.01219*, 2017.
- [66] S. Ahn, S. X. Hu, A. Damianou, N. D. Lawrence, and Z. Dai, “Variational information distillation for knowledge transfer,” in *Proceedings of the IEEE/CVF Conference on Computer Vision and Pattern Recognition*, 2019, pp. 9163–9171.
- [67] W. Park, D. Kim, Y. Lu, and M. Cho, “Relational knowledge distillation,” in *Proceedings of the IEEE/CVF Conference on Computer Vision and Pattern Recognition*, 2019, pp. 3967–3976.
- [68] B. Peng, X. Jin, J. Liu, D. Li, Y. Wu, Y. Liu, S. Zhou, and Z. Zhang, “Correlation congruence for knowledge distillation,” in *Proceedings of the IEEE/CVF International Conference on Computer Vision*, 2019, pp. 5007–5016.
- [69] Y. Tian, D. Krishnan, and P. Isola, “Contrastive representation distillation,” *arXiv preprint arXiv:1910.10699*, 2019.
- [70] J. Kim, S. Park, and N. Kwak, “Paraphrasing complex network: Network compression via factor transfer,” *arXiv preprint arXiv:1802.04977*, 2018.
- [71] J. Yim, D. Joo, J. Bae, and J. Kim, “A gift from knowledge distillation: Fast optimization, network minimization and transfer learning,” in *Proceedings of the IEEE Conference on Computer Vision and Pattern Recognition*, 2017, pp. 4133–4141.
- [72] Y. Zhang, T. Xiang, T. M. Hospedales, and H. Lu, “Deep mutual learning,” in *Proceedings of the IEEE Conference on Computer Vision and Pattern Recognition*, 2018, pp. 4320–4328.
- [73] T. Furlanello, Z. Lipton, M. Tschannen, L. Itti, and A. Anandkumar, “Born again neural networks,” in *International Conference on Machine Learning*. PMLR, 2018, pp. 1607–1616.
- [74] Y. Aytar, C. Vondrick, and A. Torralba, “Soundnet: Learning sound representations from unlabeled video,” *arXiv preprint arXiv:1610.09001*, 2016.
- [75] A. Diba, M. Fayyaz, V. Sharma, M. M. Arzani, R. Yousefzadeh, J. Gall, and L. Van Gool, “Spatio-temporal channel correlation networks for action classification,” in *Proceedings of the European Conference on Computer Vision (ECCV)*, 2018, pp. 284–299.
- [76] R. Girdhar, D. Tran, L. Torresani, and D. Ramanan, “Distinit: Learning video representations without a single labeled video,” in *Proceedings of the IEEE/CVF International Conference on Computer Vision*, 2019, pp. 852–861.
- [77] H. Zhang, Y. Li, Y. Jiang, P. Wang, Q. Shen, and C. Shen, “Hyperspectral classification based on lightweight 3-d-cnn with transfer learning,” *IEEE Transactions on Geoscience and Remote Sensing*, vol. 57, no. 8, pp. 5813–5828, 2019.
- [78] I. Merino, J. Azpiazu, A. Remazeilles, and B. Sierra, “3d convolutional neural networks initialized from pretrained 2d convolutional neural networks for classification of industrial parts,” *Sensors*, vol. 21, no. 4, p. 1078, 2021.
- [79] J. Long, E. Shelhamer, and T. Darrell, “Fully convolutional networks for semantic segmentation,” in *Proceedings of the IEEE conference on computer vision and pattern recognition*, 2015, pp. 3431–3440.
- [80] C. R. Qi, O. Litany, K. He, and L. J. Guibas, “Deep hough voting for 3d object detection in point clouds,” in *Proceedings of the IEEE/CVF International Conference on Computer Vision*, 2019, pp. 9277–9286.
- [81] Y. Tian, D. Krishnan, and P. Isola, “Contrastive multiview coding,” *arXiv preprint arXiv:1906.05849*, 2019.
- [82] A. Newell and J. Deng, “How useful is self-supervised pretraining for visual tasks?” in *Proceedings of the IEEE/CVF Conference on Computer Vision and Pattern Recognition*, 2020, pp. 7345–7354.
- [83] T. Chen, S. Kornblith, K. Swersky, M. Norouzi, and G. Hinton, “Big self-supervised models are strong semi-supervised learners,” *arXiv preprint arXiv:2006.10029*, 2020.
- [84] B. Zhou, H. Zhao, X. Puig, S. Fidler, A. Barriuso, and A. Torralba, “Scene parsing through ade20k dataset,” in *Proceedings of the IEEE conference on computer vision and pattern recognition*, 2017, pp. 633–641.